SYNCHROTRON FREQUENCY SHIFT AS A PROBE OF THE CERN SPS REACTIVE IMPEDANCE

A. Lasheen*, T. Argyropoulos, J. F. Esteban Müller, D. Quartullo, E. Shaposhnikova, H. Timko, J. Varela Campelo, CERN, Geneva, Switzerland

Abstract

Longitudinal instability in the CERN SPS is a serious limitation for the future increase of bunch intensity required by the HiLumi LHC project. The impedance driving this instability is not known precisely and a lot of effort goes into creating an accurate impedance model. The reactive impedance of the machine can be probed by measuring the bunch length oscillations of a mismatched bunch at injection. The frequency of these oscillations as a function of intensity has a slope that depends on the reactive impedance and the emittance. Measurements were done for three values of longitudinal emittance and then compared with particle simulations based on the impedance model using particle distribution close to the measured one. Comparison of measured and calculated frequency shifts gives an estimation of the missing impedance in the model. In addition, scanning of initial emittance for diverse particle distributions in simulations shows that the frequency shift greatly depends on emittance and initial distribution. Small variations of these parameters can lead to very different results and explain partially the discrepancy between measured and calculated values of frequency shifts.

INTRODUCTION

Reference measurements were done in the past in the SPS to monitor the evolution of the impedance from 1999 and successively after the 2001 impedance reduction program. Main changes were due to the installation of extraction kickers MKE in 2003 - 2006, and their shielding later [1]. New measurements were done in 2013 [2] and 2014, not only in order to continue the reference measurements, but mainly to test the SPS impedance model needed to simulate different intensity effects observed in the SPS. Below, simulations using this model are compared to measurements in order to test the model accuracy. This will allow to have a better understanding of SPS instabilities, as well as the synchrotron frequency distribution dependence on bunch intensity and bunch length.

Voltage induced due to the reactive impedance leads to the synchrotron frequency shift. This voltage can be found as the convolution of the reactive impedance with the beam spectrum (effective impedance), and is proportional to the bunch intensity N_b. The shift consists of two parts: the incoherent shift Δf_{inc}, corresponding to the convolution of the stationary bunch spectrum, and the coherent shift Δf_{coh}, corresponding to the convolution of the perturbation spectrum with the impedance. This perturbation can be due to a shift in the bunch position ($m = 1$, dipole) or a mismatch of the bunch length ($m = 2$, quadrupole). The frequency of these oscillations can be written in the form [3]:

$$f_{s,m}(N_b) \approx m\, f_s^{(0)} + m\,\Delta f_{inc}(N_b) + \Delta f_{coh}(m, N_b), \quad (1)$$

with $f_s^{(0)}$ being the synchrotron frequency without intensity effects (first term of Eq. 3). One can then measure the oscillations of a mismatched bunch for several intensities in order to probe the effective reactive impedance. For a bunch with a parabolic line density, the dipolar incoherent and coherent frequency shifts are exactly canceling [3], making it difficult to measure intensity effects with dipole oscillations. Thus it is more practical to measure the quadrupole frequency shift.

Above transition, inductive effective impedance will produce $\Delta f_{inc} < 0$ and $\Delta f_{coh} > 0$, and vice-versa for capacitive impedance.

Below, measurements are compared to simulations and analytical calculations in order to study the effect of the different SPS impedance sources on the synchrotron frequency shift, as a function of the bunch distribution.

MEASUREMENTS

The measurements of bunch length oscillations are done in the SPS just after injection (P = 25.92 GeV/c, above transition). The RF voltage is set to a value for which the injected bunch is mismatched, allowing the bunch length to oscillate for several periods (the emittance being small enough so that the oscillations are not damped too fast because of filamentation). These measurements were done for several emittances ($\epsilon_l \in [0.1, 0.20]$ eVs), and several intensities ($N \in [1, 10] \times 10^{10}$ ppb). Dipole oscillations were damped using a phase loop in order to measure only the quadrupole oscillations (referred to as oscillations for the rest of the paper). Two optics are available in the SPS (named Q26 and Q20) with transition gamma factors $\gamma_t = 22.8$ for Q26 and $\gamma_t = 18$ for Q20, which affect the synchrotron frequency. A single RF system (200 MHz) was used in measurements, with respective voltages of $V_{Q26} = 0.9$ MV for Q26 and $V_{Q20} = 2.5$ MV or $V_{Q20} = 4.5$ MV for Q20.

For each measurement set, bunch profiles were acquired every revolution turn for 1000 turns after injection and analyzed. From the oscillations of the bunch length (defined as $\tau = 4\sigma_{RMS}$), we extract the average bunch length, the peak-to-peak amplitude and the frequency of the oscillations (via FFT). Like this we get a scatter plot of the quadrupole frequencies as a function of intensity and average bunch length $f_2(\tau, N_b)$. For a narrow frame of bunch length $\tau = \tau_0 + \Delta\tau$, we plot the quadrupole frequency as a function of intensity as in Fig. 1(bottom). The top plot corresponds to a single point of the bottom one with

* alexandre.lasheen@cern.ch

ISBN 978-3-95450-173-1

$\epsilon_l = 0.1$ eVs and $N_b \approx 1 \times 10^{10}$ ppb. We can see the frequency shift with intensity effects, and fit them with linear function $f_2(\tau = \tau_0 + \Delta\tau, N_b) = a + b \times 10^{10} N_b$.

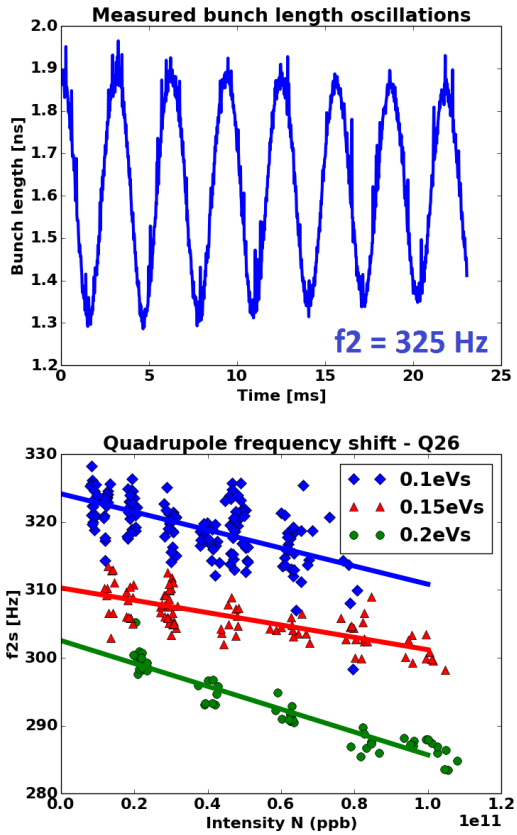

Figure 1: Bunch length oscillations for one measurement (top) and quadrupole oscillation frequencies as a function of intensity for different emittances (bottom).

The complete set of results for the 2013 and 2014 measurements are shown in the Table 1. In order to compare the Q26 and Q20 measurements, the slopes were rescaled by the factor $\sqrt{\eta_{Q26} V_{Q20}/(\eta_{Q20} V_{Q26})}$ (derived from Eq. 3), where $\eta = 1/\gamma_t^2 - 1/\gamma^2$ is the slippage factor. The averaged peak-to-peak amplitude of the oscillations is also included in the table in order to estimate the mismatch at injection. One can see that this amplitude is increasing with the average bunch length, showing that the mismatch is larger for longer bunches (Fig. 2). The standard deviation of the peak-to-peak amplitude is bigger than the one for the average bunch length, because of some scatter in the injected bunch length.

In comparison with previous reference measurements [2], the slope range for bunch lengths above 2 ns decreased from [-4.0, -3.4] Hz/$N_b \times 10^{-10}$ to [-1.68, -0.91] Hz/$N_b \times 10^{-10}$, showing a decrease of the inductive impedance due to the shielding of MKE kickers between 2009 and 2013.

PARTICLE SIMULATIONS

Simulations were done with the BLonD tracking code [4], created at CERN for multi-particle simulations with intensity

Table 1: Measurement Results (Scaled to Q26(0.9))

Optics (voltage [MV])	Average bunch length [ns]	Av. peak-peak amplitude [ns]	Slope [Hz/Nb] $\times 10^{-10}$
Q26(0.9)	1.60 ± 0.02	0.53 ± 0.06	−1.33 ± 0.07
Q26(0.9)	2.09 ± 0.02	0.70 ± 0.08	−0.91 ± 0.05
Q26(0.9)	2.07 ± 0.01	0.76 ± 0.05	−1.40 ± 0.06
Q26(0.9)	2.44 ± 0.01	0.79 ± 0.07	−1.68 ± 0.04
Q20(2.5)	1.48 ± 0.02	0.42 ± 0.05	−1.3 ± 0.2
Q20(2.5)	1.70 ± 0.03	0.51 ± 0.05	−0.0 ± 0.2
Q20(4.5)	1.32 ± 0.03	0.68 ± 0.07	−2.1 ± 0.2
Q20(4.5)	1.52 ± 0.03	0.86 ± 0.07	−0.5 ± 0.3

effects. The parameters for the RF system, particle distributions, impedance and method of data analysis were set in order to reproduce the measurement conditions and be comparable. The SPS impedance model used in simulations is the result of a thorough and still ongoing survey of the different devices in the machine [5]. The plot of the total reactive impedance is shown in Fig. 3. Main contributors to the reactive impedance are listed here (approximate values of the low frequency reactive impedance are given as $\Im[Z/p]$ with $p = f/f_0$, with the impedance having an approximately constant value in this range):

- RF systems (travelling wave cavities, capacitive)
- Kickers (inductive, $\Im[Z/p] \approx 5.3\,\Omega$)
- Vacuum flanges (inductive, $\Im[Z/p] \approx 0.55\,\Omega$)
- Unshielded pumping ports (inductive, $\Im[Z/p] \approx 0.2\,\Omega$)
- Space charge (capacitive, $\Im$[Z/p] $= -0.9\,\Omega$ in Q26 and $\Im$[Z/p] $= -1.0\,\Omega$ in Q20)
- Resistive wall (inductive)

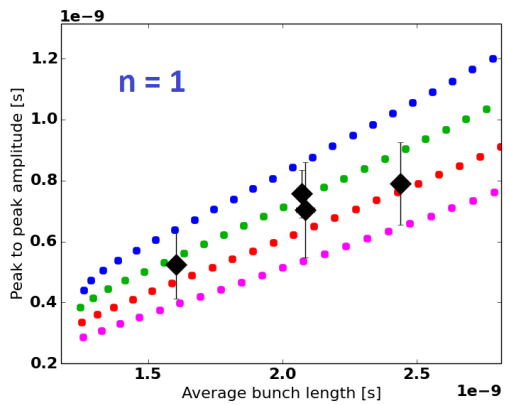

Figure 2: Peak-to-peak amplitude as a function of the average bunch length for the measurements (black) and simulations (colored) in Q26 optics.

Space charge was computed using the longitudinal space charge code LSC [6], for the averaged beam pipe geometry in the SPS and transverse bunch size (different momentum

ISBN 978-3-95450-173-1

spreads used in operation were taken into account for the dispersion). For the simulations presented here, average values of space charge impedance for the two different optics were taken.

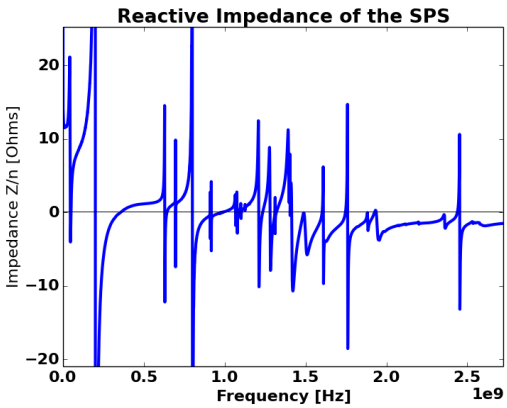

Figure 3: Reactive part of the SPS impedance model.

The exact injected distribution cannot be measured directly due to the bunch rotation used in the injector (PS), so a large range of distributions were covered in simulation to overcome these uncertainties. The injected profile was analyzed, and the closest distribution used in simulations was the binomial line density with n varying between 1 (parabolic line density without tails) and 1.5 (an increasing n gives more tails to the distribution).

$$\lambda(t) = \lambda_0 \left[1 - \left(\frac{t}{\tau_L}\right)^2\right]^n \qquad (2)$$

The momentum spread was estimated from the peak-to-peak amplitude of the bunch length oscillations. The bunch was generated in simulations in order to cover the full range of peak-to-peak amplitudes observed in measurements. This is shown in Fig. 2, where each colored point corresponds to a simulation with a different initial distributions ($n = 1$ for the profile).

In simulations, the bunch size (momentum spread and bunch length), the distribution type (different n) and the intensity were scanned. The results are shown in Fig. 4 for Q26 and Fig. 5 for Q20 (2.5 MV only; 4.5 MV giving similar results), in comparison with simulations.

The simulations show an unexpected maximum around $\tau = 1.7$ ns for which the slope is almost 0, implying that the synchrotron frequency shift is acting like there is no impedance at all! This was not seen with the Q26 measurement in 2013, as no measurements were done in this region. This was, however, observed in simulations with $\tau \approx 1.6$ ns, for which very small changes in bunch length would give very different results in the slopes. This is now understood, as this point is in a region where the slope as a function of bunch length is varying a lot. Moreover, the two measurements sets around $\tau \approx 2.1$ ns give very different results, as the slopes are also sharply changing around this bunch

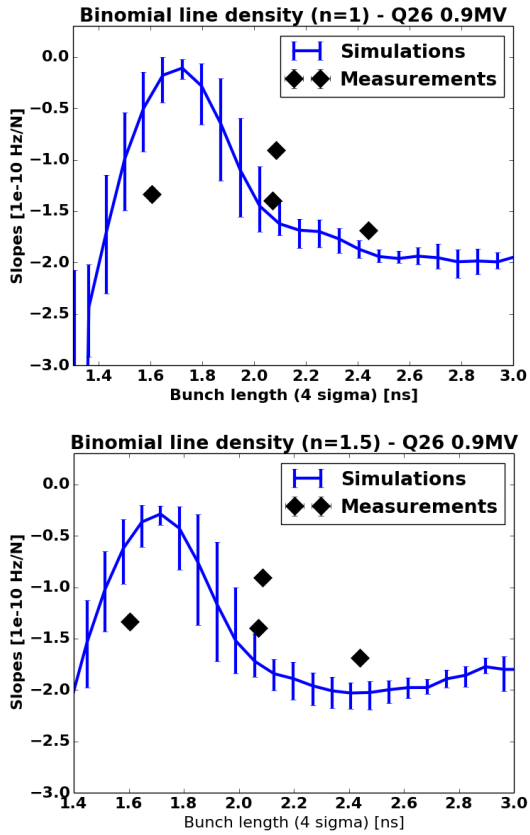

Figure 4: Slopes b of synchrotron frequency shift with intensity as a function of bunch length, comparison of simulations and measurements in Q26 for V=0.9 MV with $n = 1$ for the injected distribution.

length. Another point is that small changes in the binomial function also lead to different results for the slopes.

The errorbars correspond to the deviation in the slopes due to the different momentum spreads chosen in simulations in Fig. 2. By comparing measurements with simulations, we can see that the measurements seem to be shifted by $\approx$ 100 ps to a larger bunch length. The source of this shift could be the measurement method, with the bunch length in measurements being larger due to e.g. pick-up cable length, or that some impedance depending on bunch length is missing in the present model.

Since the previous measurements in Q26 did not cover the region where the slope is at its maximum, measurements were repeated with the operational Q20 optics. Corresponding simulations are presented in Fig. 5.

Unfortunately, these measurements were done right after the end of the long shutdown at CERN, so that it was not yet possible to achieve all the desired bunch lengths. However, we managed to have a few measurements around $\tau = 1.7$ ns. Like in the measurements section, the slopes were scaled to the Q26 (0.9MV) settings to be comparable, but simulations were done under the same conditions as in measurements in the Q20 optics. They show the same pattern, with the slope being even positive at the maximum. Due to the small

ISBN 978-3-95450-173-1

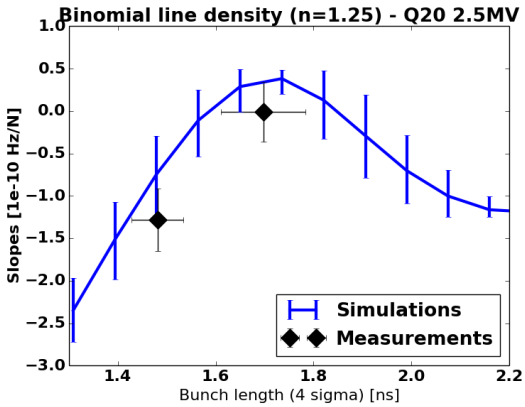

Figure 5: Slopes b of synchrotron frequency shift with intensity as a function of bunch length, comparison of simulations and measurements in Q20 for V=2.5 MV with $n = 1.25$ for the injected distribution.

number of measurements, the uncertainties are bigger and more measurements would be needed.

One additional motivation for these measurements was the fact that controlled emittance blow-up in the SPS is done by applying RF noise with a fixed band-width relative to the synchrotron frequency. These simulations show that this synchrotron frequency shift is varying a lot as a function of the bunch length and should be taken into account in operation.

QUADRUPOLE FREQUENCY SHIFT

In order to understand the source of this bunch length dependence, an analytical calculation of the quadrupolar frequency shift was done. First, the incoherent frequency was computed from potential well distortion [7]. The shift depends on the amplitude of the oscillations in longitudinal phase space $\hat{\tau}$. The effective impedance Z_1 for the incoherent shift is computed for a parabolic stationary spectrum using the following formulas:

$$f_s^2(N_b,\hat{\tau}) \approx f_{s0}^2\left(1-\frac{(2\pi h f_0\hat{\tau})^2}{16}\right)^2\left(1+\frac{eN_b f_0 Z_1}{hV_0\cos\phi_s}\right), \quad (3)$$

$$Z_1 = \int_{-\infty}^{+\infty}\frac{df}{f_0}\,\sigma_0\Im(Z(f))\frac{J_1(f\hat{\tau})}{f_0\hat{\tau}/2}, \quad (4)$$

where f_0 is the revolution frequency, f_{s0} the synchrotron frequency for the small amplitude of oscillations, h the harmonic number, V_0 the RF voltage, ϕ_s the synchronous phase, σ_0 the stationary bunch spectrum, and $J_\nu(x)$ the Bessel function of order ν.

Next, the coherent frequency shift is computed as in [8] (assuming again a parabolic bunch) and applied to the incoherent frequency f_s in order to obtain the final quadrupolar frequency containing both contributions.

$$f_2(N_b) \approx 2f_s + \frac{3\Gamma(5/2)N_b e^2\eta}{4\pi\sqrt{\pi}Ef_s\tau_L^3}\left(\frac{Z}{p}\right)_{eff}, \quad (5)$$

$$\left(\frac{Z}{p}\right)_{eff} = \frac{\sum_{p=-\infty}^{p=+\infty}h_2\frac{Z}{p}}{\sum_{p=-\infty}^{p=+\infty}h_2}; h_2(\omega_p) = \frac{\left[J_{5/2}(\omega_p\tau_L)\right]^2}{\omega_p\tau_L}, \quad (6)$$

where $\Gamma(5/2)$ is the gamma function, e is the elemental charge, E the beam energy, τ_L the binomial bunch length parameter as in Eq. 2, h_2 the perturbation spectrum for the quadrupole mode, and finally $\omega_p = p2\pi f_0$.

From Eq. 4 and Eq. 6, we can compute the effective impedances in order to obtain the incoherent and coherent shifts as a function of bunch length. The results are shown in Fig. 6, for the different sources of impedance. The analytical slope is finally computed by comparing the quadrupole frequency with (f_2) and without ($2f_s^{(0)}$) intensity, and results are given in Fig. 7 (top).

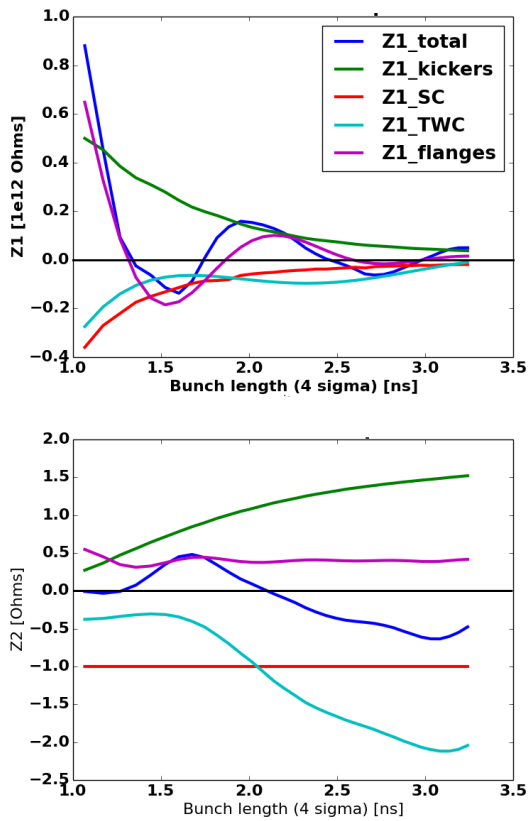

Figure 6: Effective impedance for the main impedance sources as a function of bunch length for the incoherent (top, Z_1) and coherent (bottom, Z_2) shifts (same color code, SC corresponds to space charge and TWC to the impedance of the RF systems). The slopes of incoherent and coherent shifts are directly proportional to these effective impedances.

For the effective impedance used in the incoherent shift, one can see a clear dependence on bunch length, varying from positive to negative, with a maximum capacitive impedance around $\tau \approx 1.6$ ns (implying a positive slope, for the same bunch length as the maximum in simulations and measurements!). The impedance of vacuum flanges, which is expected to be inductive, can also act as capacitive, depending on the bunch length. The other impedances vary with

ISBN 978-3-95450-173-1

bunch length but remain capacitive or inductive. This can be seen in Fig. 7 (bottom) from the fact that for $\tau \approx 1.6$ ns bunch length, the negative spectrum (parabolic bunch) is sampling a high value of inductive impedance, which is then converted into capacitive effective impedance.

Moreover, the maximum of the effective impedance causing coherent shift (Z_2) is around the same bunch length as the minimum of the effective impedance causing incoherent shift (Z_1). Since $Z_2 > 0$ at the maximum, the impedance is inductive, hence resulting in a positive slope of coherent shift. It seems though that the shape of $Z_2(\tau)$ is mainly due to the kickers and the RF systems' impedance, since effective impedances are varying a lot in this range.

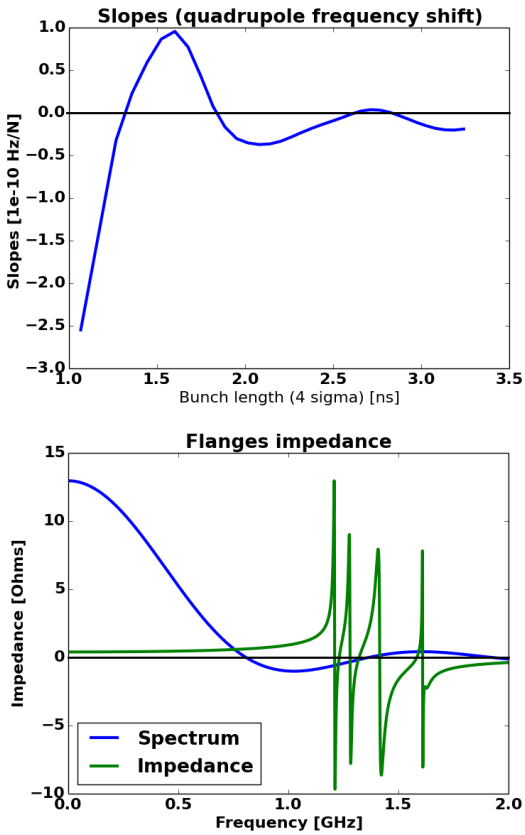

Figure 7: Top: Slopes of the synchrotron frequency shift as a function of bunch length for parabolic line density. Bottom: Spectrum and reactive impedance of flanges for the maximum slope value.

The shape of the curve resembles the one from simulations (Fig. 4). The maximum is also around the same bunch length $\tau \approx 1.6 - 1.7$ ns, and the relative values with respect to the maximum are very close to simulations. One can see though an important offset of the values of the slope (around 1×10^{10} [Hz/N$_b$]) which is not understood yet. Note that analytical formulas are valid for small perturbations only, but large deviations exist in measurements. So it is more accurate to compare measurements to simulations rather than analytical formulas.

CONCLUSIONS

A dependence of the synchrotron frequency shift on bunch length was measured in the SPS and reproduced in simulations. The results are in good agreement with the actual SPS impedance model. The reason for this dependence was studied and it has been shown that the interaction of a parabolic bunch spectrum with the impedance of the SPS vacuum flanges caused an incoherent frequency shift. This shift can be inductive or capacitive as a function of the bunch length, and may lead to the cancellation of the slope at certain bunch length. Further studies are planned in order to understand the discrepancy between theory and what is observed in measurements and simulations. New methods are also planned, like applying a fast voltage increase as a source of the mismatch to a matched bunch. Like this, one can have a better control of the perturbation and initial bunch distribution. Experiments at flat top energy, where the space charge impedance is negligible, can help to study the effect of space charge on the synchrotron frequency shift.

ACKNOWLEDGMENTS

We would like to thank the members of the BE/RF/BR and BE/ABP/HSC sections and more particularly T. Bohl for his support during measurements, C. Zannini and B. Salvant for providing elements of the impedance model, as well as the operation team for their assistance during machine development sessions. Thanks also to L. Wang for providing the LSC code and instructions.

REFERENCES

[1] E. Shaposhnikova et al., "Reference Measurements of the Longitudinal Impedance in the CERN SPS", PAC'09, Vancouver, BC, Canada, (2009).

[2] T. Argyropoulos et al., "Reference Measurements of the Longitudinal Impedance", *Meetings of the LIU-SPS BD WG*, CERN, `http://cern.ch/spsu/`

[3] J. L. Laclare, "Bunched Beam Coherent Instabilities", CERN 87-03, p.264, *CAS Proceedings*, (1987).

[4] BLonD, Beam Longitudinal Dynamics code: `http://blond.web.cern.ch/`

[5] B. Salvant, J. Varela Campelo, C. Zannini, "SPS Impedance Model Update", *Meetings of the LIU-SPS BD WG*, CERN, `http://cern.ch/spsu/`

[6] L. Wang, "The geometry effect of the space charge impedance LSC code", *ICFA mini-Workshop on "Electromagnetic wake fields and impedances in particle accelerators"*, Erice, Italy, (2013).

[7] K. Y. Ng, *Physics of Intensity Dependent Beam Instabilities*, Ed. World Scientific Publishing, (2006).

[8] A. Chao, *Physics of Collective Beam Instabilities in High Energy Accelerators*, Ed. John Wiley & Sons, (1993).

ISBN 978-3-95450-173-1